



# THE UNIVERSITY *of* EDINBURGH

## Edinburgh Research Explorer

### **Survival and Enhancing Fraction (enf) in Glioblastoma Multiforme (GBM)**

**Citation for published version:**

Mills, S, G, T, G, B, Gjm, P & A, J 2017, 'Survival and Enhancing Fraction (enf) in Glioblastoma Multiforme (GBM)' *Radiology and Diagnostic Imaging*, vol. 1, no. 3. DOI: 10.15761/RDI.1000118

**Digital Object Identifier (DOI):**

[10.15761/RDI.1000118](https://doi.org/10.15761/RDI.1000118)

**Link:**

[Link to publication record in Edinburgh Research Explorer](#)

**Document Version:**

Publisher's PDF, also known as Version of record

**Published In:**

*Radiology and Diagnostic Imaging*

**General rights**

Copyright for the publications made accessible via the Edinburgh Research Explorer is retained by the author(s) and / or other copyright owners and it is a condition of accessing these publications that users recognise and abide by the legal requirements associated with these rights.

**Take down policy**

The University of Edinburgh has made every reasonable effort to ensure that Edinburgh Research Explorer content complies with UK legislation. If you believe that the public display of this file breaches copyright please contact [openaccess@ed.ac.uk](mailto:openaccess@ed.ac.uk) providing details, and we will remove access to the work immediately and investigate your claim.



# Survival and enhancing fraction (EnF) in glioblastoma multiforme (GBM)

SJ Mills<sup>1,2\*</sup>, Thompson G<sup>2,3</sup>, Buonaccorsi G<sup>2</sup>, Parker GJM<sup>2</sup> and Jackson A<sup>2</sup>

<sup>1</sup>Department of Neuroradiology, The Walton Centre NHS Foundation Trust, Lower Lane, Liverpool, UK

<sup>2</sup>CRUK-EPSRC Cancer Imaging Centre in Cambridge and Manchester and Imaging Sciences, Institute of Population Health, University of Manchester, UK

<sup>3</sup>Centre for Clinical Brain Sciences, The University of Edinburgh, Chancellor's Building, 49 Little France Crescent, Edinburgh, UK

## Abstract

In GBM, enhancing fraction derived from the initial area under the contrast agent concentration curve (*LAUC*),  $\text{EnF}_{LAUC60}$ , correlates with the MRI parameter  $K^{\text{trans}}$  (contrast agent transfer coefficient). Thresholding voxels as enhancing when  $LAUC60 > 2.5 \text{ mMol.s}$  ( $\text{EnF}_{LAUC60 > 2.5}$ ) separates high from low grade glioma. The objectives were to evaluate the feasibility of deriving a signal intensity based enhancing fraction ( $\text{EnF}_{SI}$ ), assess its relationship with  $\text{EnF}_{LAUC60}$  measures and examine relationships with survival in GBM.

30 GBM had pre-operative pre and post-contrast  $T_1$ -weighted imaging and a  $T_1$ -DCE-MRI protocol.  $\text{EnF}_{LAUC60 > 0}$  and  $\text{EnF}_{LAUC60 > 2.5}$  were generated from  $LAUC_{60}$  maps.  $\text{EnF}_{SI}$  was derived from pre and post-contrast  $T_1$ -weighted sequences. Bland/Altman plots assessed agreement between  $\text{EnF}$  measures. A multivariate Cox regression analysis examined the prognostic value of  $\text{EnF}$  measures.

The mean difference between  $\text{EnF}_{LAUC60 > 0}$  and  $\text{EnF}_{SI}$  was 0.0378 (range -0.112-0.264, std. dev 0.07573) and between  $\text{EnF}_{LAUC60 > 2.5}$  and  $\text{EnF}_{SI}$  was -0.2492 (range -0.6096-0.2416, std. dev 0.2154).  $\text{EnF}_{SI}$  demonstrated good correlation with both  $\text{EnF}_{LAUC60 > 0}$  and  $\text{EnF}_{LAUC60 > 2.5}$  but was not directly interchangeable with either metric. Increased  $\text{EnF}_{LAUC60 > 0}$  was associated with prolonged survival ( $p=0.008$ ). A non-significant trend was seen with  $\text{EnF}_{SI}$  ( $p=0.061$ ).

$\text{EnF}_{SI}$  can be derived from conventional imaging and correlates with  $LAUC60$  based metrics. Furthermore, enhancing fraction conveys potential prognostic information in GBM.

## Introduction

The potential of enhancing fraction (EnF) in predicting cancer outcome was first described in epithelial ovarian carcinoma where a CT based metric was found to predict clinical outcome following first line chemotherapy [1]. An MRI based measure of EnF has been shown to provide clinical information in glioma [2,3]. The commonest approach to calculating EnF from MRI is to use the initial area under the concentration time curve ( $IAUC_{60}$ ) derived from dynamic contrast enhanced MRI (DCE-MRI) and to measure the proportion of voxels within a tumour with a measurable  $IAUC$  ( $> 0 \text{ mMol.s}$ ) [2,3]. The application of a thresholding technique to EnF allows for the distinction between low and high grade glioma [3]. EnF has been shown to correlate with the established DCE-MRI derived parameters  $v_p$  (in low grade glioma) and  $K^{\text{trans}}$  (in glioblastoma multiforme, GBM) [2]. The present technique for measuring EnF requires a DCE-MRI acquisition, calculation of pixel by pixel contrast concentration time course curves providing parametric maps of  $IAUC_{60}$ . Although  $IAUC_{60}$  is considered to be a more reliable, reproducible and robust measure than some pharmaco-kinetic modelling parameters such as  $v_p$  [4], the requirement of a DCE-MRI acquisition and post processing analysis limits its use in the routine clinical setting.

Baseline, pre-operative measurements of blood volume (derived from both  $T_1$  DCE and DSC imaging techniques) and  $K^{\text{trans}}$  (from  $T_1$

DCE) [5-11] have shown potential in predicting survival in GBM. But as stated above, these techniques can require lengthy acquisitions and complex post processing analysis, which limits their application in the clinical setting. To date, the clinical application of these metrics focuses predominantly on guiding the surgeon in targeting biopsy, evaluating for malignant de-differentiation and attempting to differentiate from treatment effect and tumour progression. In a research setting, there is some utilisation of these metrics as potential surrogate biomarkers in monitoring treatment response in clinical trials of novel therapeutic agents [12].

The aims of this study were: 1) to establish the feasibility of acquiring a measure of enhancing fraction based on changes in signal intensity ( $\text{EnF}_{SI}$ ); 2) to compare this with the more established  $IAUC_{60}$  (both  $\text{EnF}_{LAUC60 > 0}$  and  $\text{EnF}_{LAUC60 > 2.5}$ ) based technique and 3) to assess the relationship of different measurements of EnF with survival in a cohort of GBM patients.

**Correspondence to:** Mills SJ, Department of Neuroradiology, The Walton Centre NHS Foundation Trust, Lower Lane, Liverpool, UK, E-mail: Samantha.mills@thewaltoncentre.nhs.uk

**Received:** October 26, 2017; **Accepted:** November 15, 2017; **Published:** November 22, 2017

## Methods

### Patients

The study had local ethical approval from the North-West Manchester Research and Ethics Committee and all patients provided written informed consent prior to imaging. All methods were performed in accordance with the relevant guidelines and regulations. Patients were identified via the weekly neuro-oncology multi-disciplinary team meetings at Salford Royal NHS Foundation Trust and inclusion criteria included patients over the age of 18 years with subsequent histologically confirmed grade IV GBM according to World Health Organisation (WHO) criteria. All imaging was performed prior to surgery. All patients received corticosteroids treatment for a minimum of 48 hours prior to imaging as the sole form of treatment prior to imaging. The minimum time period of 48 hours was chosen to ensure the steroid effects on perfusion/enhancement had plateaued by the point of imaging. Exclusion criteria included patients with contra-indication to MRI of any sort, poor renal function (contra-indicating gadolinium administration) and subsequent failure to have confirmatory diagnosis of GBM on histology.

### Data acquisition

Imaging was performed on 3 Tesla Philips Achieva system (Philips Healthcare, Best, Netherlands) at the University of Manchester Magnetic Resonance Imaging Facility (Salford Royal Foundation Trust Hospital, Salford), using a SENSE 8-channel head coil. The DCE-MRI protocol images were acquired in a sagittal oblique orientation, which incorporated the internal carotid artery for measurement of an arterial input function (AIF) during the dynamic sequence and provided geometrically matched pre and post contrast  $T_1$ -weighted sequences for definition of the tumour volume of interest ( $VOI_{tumour\_coreoblique}$ ). In addition, axial pre and post contrast  $T_1$ -weighted sequences were acquired in keeping with our institution's routine tumour imaging protocol. Sequences included: 1) An axial pre contrast  $T_1$ -weighted spin echo sequence (TR 10 ms, TE 500 ms, slice thickness 4.0 mm, 256 x 256 matrix). 2) A sagittal oblique pre contrast  $T_1$ -weighted sequence (TR 9.3 ms, TE 4.6 ms, slice thickness 4.2 mm, 128 x 128 matrix). 3) Three sagittal oblique pre-contrast spoiled fast field echo ( $T_1$ -FFE spoiled gradient echo) sequences with different flip angles ( $2^\circ$ ,  $10^\circ$  and  $16^\circ$ ) for calculation of baseline  $T_1$  maps (TR 3.5 ms, TE 1.1 ms, slice thickness 4.2 mm, 128 x 128 matrix) using the standard variable flip angle relationship [13]. 4) A sagittal oblique dynamic, contrast enhanced acquisition series with identical acquisition parameters as the variable flip angle baseline  $T_1$  measurement, consisting of 100 volumes with temporal spacing of approximately 3.4 seconds. Gadolinium-based contrast agent (Gd-DTPA-BMA; Omniscan, GE Healthcare, Oslo, Norway) was injected as a bolus of 3 ml, at 15  $mls^{-1}$ , at a dose of 0.1  $mmolkg^{-1}$  of body weight after acquisition of the fifth image volume. 5) A sagittal oblique post contrast  $T_1$ -weighted sequence (TR 9.3 ms, TE 4.6 ms, slice thickness 4.2 mm, 128 x 128 matrix). 6) An axial post contrast  $T_1$ -weighted spin echo sequence (TR 10 ms, TE 500 ms, slice thickness 4.0 mm, 256 x 256 matrix)

All sagittal oblique acquisitions were co-aligned at the point of data acquisition.

### Data analysis

VOIs were manually defined by an experienced radiologist (SJM) using a technique which has previously shown good inter-observer agreement (Intraclass Correlation Coefficient > 0.94) [14] VOIs (Figure 1) included a tumour VOI on the sagittal oblique post contrast

### Comparison of methods of Enhancing Fraction Measurement

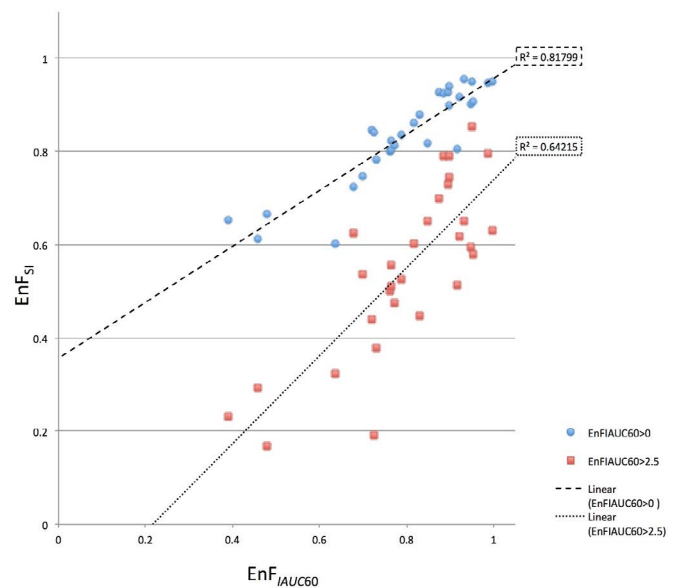


**Figure 1.** Scatter plot of  $EnF_{IAUC60>0}$  (blue circles) and  $EnF_{IAUC60>2.5}$  (red triangles) versus  $EnF_{Si}$  for all patients. There is a significant correlation between  $EnF_{Si}$  and both DCE-MRI derived parameters ( $EnF_{IAUC60>0}$ :  $\square = 0.870$ ,  $p < 0.001$  and  $R^2 = 0.818$  and  $EnF_{IAUC60>2.5}$ :  $\square = 0.744$ ,  $p < 0.001$  and  $R^2 = 0.642$ ).

$T_1$ -weighted image ( $VOI_{tumour\_coreoblique}$ ), a tumour VOI on the axial post contrast  $T_1$ -weighted image ( $VOI_{tumour\_coreaxial}$ ) and a VOI of contralateral normal appearing white matter (NAWM) on the axial post contrast  $T_1$ -weighted image ( $VOI_{NAWM\_axial}$ ). A slice including the internal carotid artery was identified by the same radiologist to allow the generation of automated arterial input functions for the DCE-MRI analysis [15]. Post processing analysis was performed using in-house software (MaDyM – Manchester Dynamic Modelling) and the extended Tofts and Kermode pharmacokinetic model [16] and parametric maps of  $IAUC_{60}$  were generated.

MATLAB (The Mathworks, Natick, Massachusetts, USA) was used for calculating all measures of enhancing fraction. For each tumour  $EnF_{IAUC60>0}$  was calculated by dividing the volume of voxels with an  $IAUC_{60} > 0$   $mMol.s$  by the total volume of the  $VOI_{tumour\_coreoblique}$ .  $EnF_{IAUC60>2.5}$  was calculated by dividing the volume of voxels with an  $IAUC_{60} > 2.5$   $mMol.s$  by the total volume of the  $VOI_{tumour\_coreoblique}$ . The change in signal intensity between pre and post contrast imaging was calculated for all voxels in both  $VOI_{tumour\_axial}$  and  $VOI_{NAWM\_axial}$ .  $EnF_{Si}$  was calculated by measuring the volume of voxels with enhancement greater than the mean change in signal intensity in NAWM + 2 standard deviations, divided by the total volume of voxels in the  $VOI_{tumour\_axial}$ .

### Statistical analysis

All statistical analysis was performed using SPSS version 15.0 (SPSS Inc., Chicago, USA). Scatter plots of  $EnF_{IAUC60>0}$  and  $EnF_{IAUC60>2.5}$  versus  $EnF_{Si}$  were generated. Agreement between the two measures of  $EnF$  ( $EnF_{IAUC60>0}$  and  $EnF_{IAUC60>2.5}$  versus  $EnF_{Si}$ ) were assessed with Bland-Altman plots and a paired  $t$ -test on the mean observed differences between the two measures versus a mean difference of zero was performed to assess the probability of inherent bias in one method as compared with standard [17,18]. In addition, intraclass correlation analysis was performed as an alternative method of comparing the methodologies [19]. A further analysis of the relationship with all

measures of EnF, age, pre-surgical tumour volume, treatment (initial chemoradiotherapy versus palliative radiotherapy) and patient survival using a multivariate Cox regression analysis was performed on a subset of patients with newly presenting GBM. Patients with recurrent GBM were excluded.

The datasets generated during and/or analysed during the current study are available from the corresponding author on reasonable request.

## Results

30 patients were included in the initial aspect of the study, comparing the different methods of EnF measurement (11 female, 19 males, mean age 59 years, age range 18-76 years). In the subsequent survival analysis, 1 patient with recurrent GBM was excluded. 1 patient was lost to follow up, but included in the analysis and censored, in accordance with standard Cox regression survival analysis.

The scatter plots for both  $EnF_{IAUC60>0}$  and  $EnF_{IAUC60>2.5}$  versus  $EnF_{SI}$  are shown in Figure 1 and the Bland Altman plots in Figure 2. The results for the Bland Altman analysis are presented in Table 1. For  $EnF_{IAUC60>0}$  versus  $EnF_{SI}$ , the paired *t*-test demonstrated a significant difference between the mean difference between measures and a mean difference of zero,  $p = 0.011$ . For  $EnF_{IAUC60>2.5}$  versus  $EnF_{SI}$ , the paired *t*-test demonstrated a significant difference between the mean difference between measures and a mean difference of zero,  $p < 0.001$ . Excellent intraclass correlation coefficients were demonstrated between  $EnF_{SI}$  and both *IAUC60* based measurements of EnF ( $EnF_{IAUC60>0}$  ICC = 0.909 and  $EnF_{IAUC60>2.5}$  ICC = 0.883), indicating ‘almost perfect’ consistency of between  $EnF_{SI}$  and  $EnF_{IAUC60>0}$  [19].  $EnF_{SI}$  had a tendency to measure slightly lower than  $EnF_{IAUC60>0}$  and markedly higher than  $EnF_{IAUC60>2.5}$  (Figure 1). The lowest values of  $EnF_{IAUC60>0}$  (less than approximately 0.60) demonstrated the greatest discrepancy between  $EnF_{IAUC60>0}$  and  $EnF_{SI}$  measures (Figure 3).

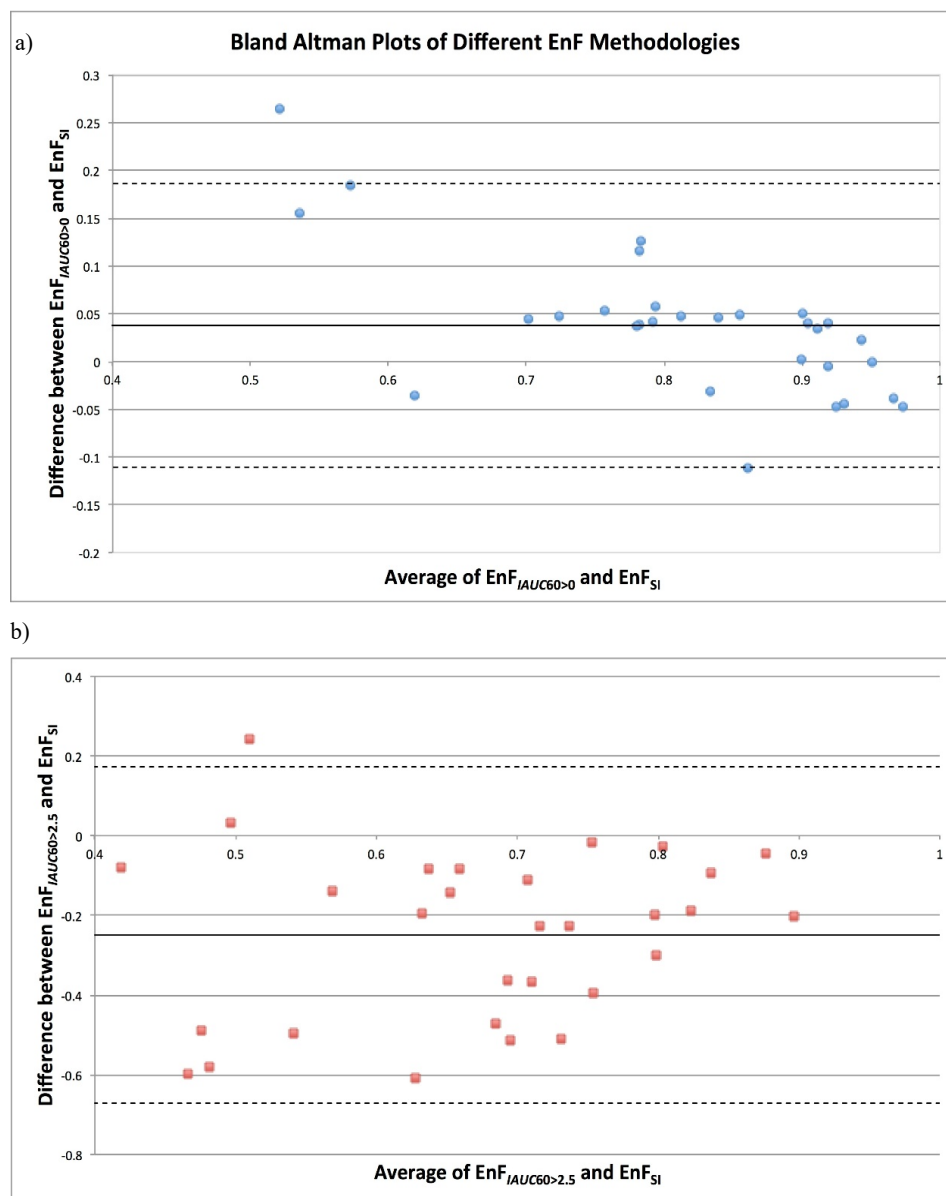


**Figure 2.** Bland Altman Plot of Average Enhancing Fraction determined by a)  $EnF_{IAUC60>0}$  and  $EnF_{SI}$  versus the mean difference ( $EnF_{IAUC60>0}$  minus  $EnF_{SI}$ ) between the two measures and b)  $EnF_{IAUC60>2.5}$  and  $EnF_{SI}$  versus the mean difference ( $EnF_{IAUC60>2.5}$  minus  $EnF_{SI}$ ) between the two measures.

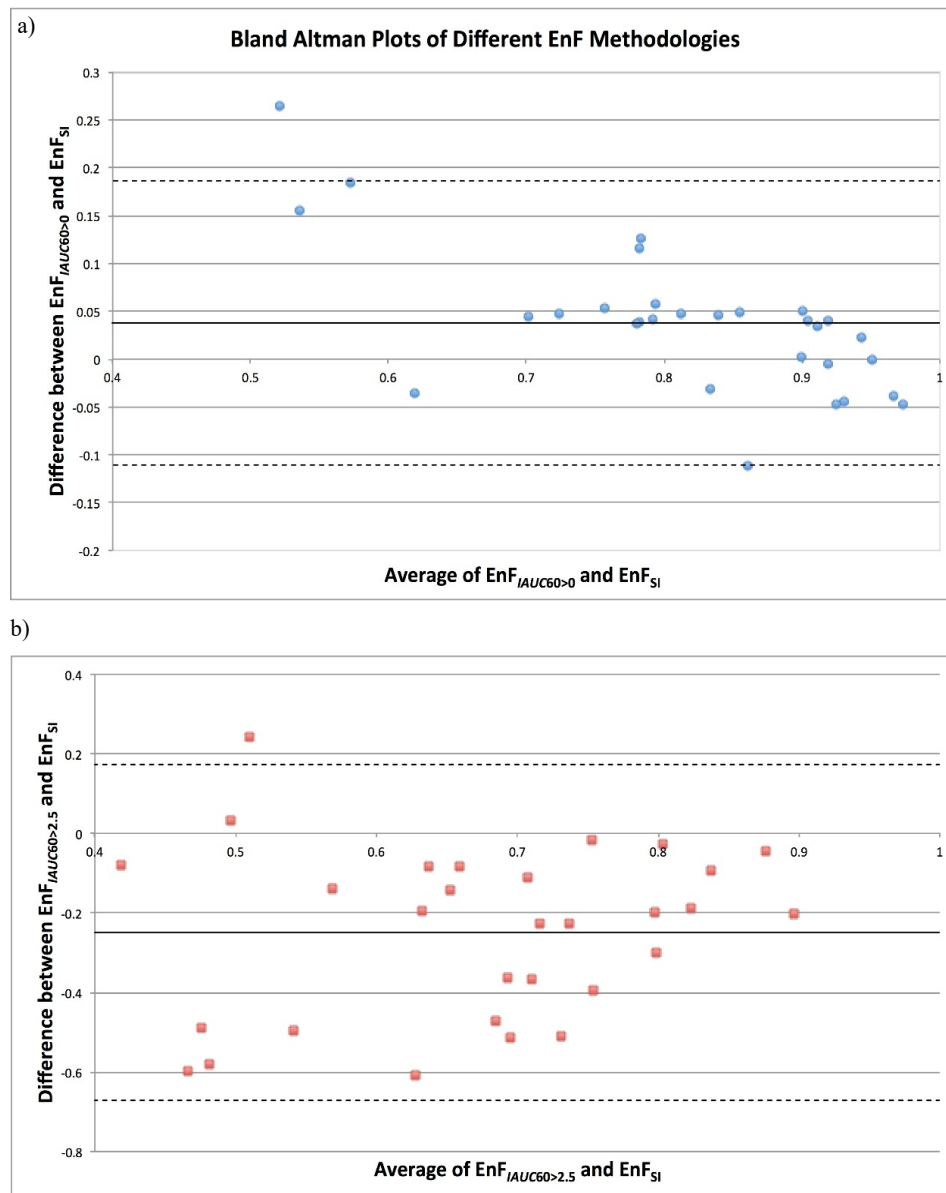


**Figure 3.** Scatter plot of a)  $EnF_{IADC60>0}$  and patient survival, linear regression analysis shows increased survival with increased  $EnF_{IADC60>0}$  ( $p=0.008$ ) and b)  $EnF_{S1}$  and patient survival. A non-significant trend is seen with increased survival with increased  $EnF_{S1}$  ( $p=0.061$ ).

**Table 1.** Cox multivariate significance levels for relationship between parameters and patient overall survival. \*\* Significance taken as  $p<0.01$

Parameter	Cox Multivariate Significance Level (p=)
Pre-operative tumour volume	0.101
Age	0.15
Treatment regime	0.261
$EnF_{S1}$	0.061
$EnF_{IADC60>0}$	0.008**
$EnF_{IADC60>2.5}$	0.384

The Cox multivariable analysis results are shown in table 1. Only  $EnF_{IADC60>0}$  ( $p=0.008$ ) and age ( $p=0.01$ ) demonstrated significant relationships with overall survival (Figure 3). A trend was seen with increasing  $EnF_{S1}$  and patient survival, but this failed to reach significance ( $p = 0.061$ , Figure 4). Survival did not differ between patients receiving chemoradiotherapy or palliative radiotherapy ( $p=0.261$ ). Neither pre-treatment tumour volume or patient age demonstrated a significant relationship with survival ( $p=0.101$  and  $p=0.15$ , respectively).

## Discussion

EnF is a relatively recently described parameter [2,3,20,21]. A CT variant of this measure has shown potential in predicting disease free survival and time to progression in patients with ovarian carcinoma [1]. The technique used in this study was simple, using only post contrast CT images and calculating EnF by classifying voxels as enhancing if the Hounsfield unit measure for a given voxel was greater than a set threshold. A number of patients with cerebral tumours will have a CT scan as their initial investigation, but the imaging modality of choice for brain tumour characterisation is an MRI scan and therefore the ability to derive a signal intensity based MRI measure of EnF was assessed in the current study as opposed to a CT based measure. A study of DCE-MRI derived EnF in glioma has shown the use of thresholding allows the distinction between histological grade of tumour [3]. In the unthresholded form,  $EnF_{IADC60>0}$  correlated with  $v_p$  in low grade tumours and  $K^{trans}$  in GBM [2]. These latter studies have all required a DCE-MRI acquisition in order to derive EnF, thus limiting the translation

of this research into the clinical setting. The ability to derive EnF from conventional pre and post contrast weighted imaging makes it a much more attractive parameter for clinical use. This study demonstrates that it is feasible to obtain a signal intensity based measure of EnF from routine conventional imaging, which is comparable with that derived from DCE-MRI data.

The EnF measures are not directly interchangeable;  $EnF_{SI}$  having a tendency to measure slightly lower than  $EnF_{IAUC60>0}$  and markedly higher than  $EnF_{IAUC60>2.5}$  (Figure 1). This likely reflects the difference in thresholding between the techniques. The  $EnF_{IAUC60>0}$  metric has no thresholding applied at all and merely identifies a voxel as enhancing due to contrast agent being measurable.  $EnF_{SI}$  is thresholded relative to NAWM, thereby a voxel is only considered to be enhancing if there is an increase in T1 signal intensity that is greater than would be expected in NAWM.  $EnF_{IAUC60>2.5}$  is thresholded to a level that provides maximum discrimination between grade II and grade IV gliomas.

Other groups have previously used signal intensity based measures to assess enhancement in glial tumours [22-24] but these have predominantly focused on assessing the intensity of enhancement, rather than the proportion of enhancement. Serial studies of such metrics have shown potential in predicting which low grade gliomas will subsequently undergo malignant transformation [24] and, in high grade gliomas, have been shown to correlate with the volume of surrounding oedema [23]. Unlike the thresholded measure of EnF ( $EnF_{IAUC60>2.5}$ ) these measures do not distinguish between histological grade of tumour [3,22]. Studies of subjective semi-quantitative [25,26] and planimetry volume [27] measures of tumour "necrosis", defined as non-enhancement, have shown shorter survival in patients with larger necrotic volumes, and this is concordant with our findings. More recently, the change in T1 signal measured on conventional post contrast sequences on serial imaging in bevacizumab treated recurrent GBM has shown value in predicting disease progression [28].

There are potential limitations in using a signal intensity based method for calculating EnF. Unlike CT, the relationship between signal intensity and contrast agent concentration on MRI is nonlinear. However, the measurement of EnF does not require an estimation of the degree of intensity of enhancement, but merely a binary measure of whether it is present or not in order to calculate the proportion of tumour that enhances. Normalising the change in signal intensity with that seen in contralateral NAWM improves the specificity so that only changes in signal intensity greater than those seen in NAWM are classified as enhancing. This normalisation technique should also help overcome variations in signal intensity that may occur between subjects, scanners, acquisition sequences and centres.

In this study,  $EnF_{IAUC60>0}$  alone demonstrated a significant relationship with overall patient survival and this was irrespective of treatment, pre-operative tumour volume and age. The lack of a difference in survival between full chemoradiotherapy regime and palliative radiotherapy alone is interesting. This may reflect an unconscious bias by the clinicians to palliate patients with larger, more necrotic tumour rather than subject those individuals to a full chemoradiotherapy regime, although no relationship between pre-operative tumour volume and survival was found in our small study. A trend of increasing  $EnF_{SI}$  and prolonged survival was noted but failed to reach significance. There are a number of differences between these two EnF measures.  $EnF_{SI}$  is normalised to contralateral normal appearing white matter, and is therefore more likely to represent pathological 'enhancement' as any 'enhancement' similar to that seen in normal brain is excluded as 'non-enhancing'. Due to the technique and post-processing analysis for measurement  $EnF_{IAUC60>0}$  no normalisation with contralateral

normal appearing white matter could be made, therefore measurement of EnF via this method classifies voxels as enhancing if they contain any contrast agent within them, even within the normal vascular space (as in normal brain tissue) and therefore may give a higher measure of EnF when compared to a technique which is adjusted to normal brain tissue. Furthermore, the  $EnF_{IAUC60>0}$  parameter is obtained from a volumetric dataset, whilst the  $EnF_{SI}$  is derived from non-volumetric 4 mm conventional imaging slices. No attempt was made during the conventional imaging acquisition to overcome the automatic scanner gain function and therefore variability in the measures of signal intensity may have occurred between pre and post contrast imaging for each patient, but this is unlikely to have had a significant impact thanks to the test for signal intensity enhancement difference from NAWM, which provides normalisation for changes of intensity scale. The failure for  $EnF_{SI}$ , unlike  $EnF_{IAUC60>0}$  to significantly relate to survival, may reflect the small number of patients in this current study. Whilst DCE-derived EnF is likely to be a more robust and reliable parameter than  $EnF_{SI}$ ,  $EnF_{SI}$  has the advantage of being available from conventional pre and post contrast T1-weighted sequences which are part of routine clinical imaging and do not require additional T1 mapping sequences and a DCE-acquisition and the associated complex pharmacokinetic post-processing making this technique a more desirable tool for the routine clinical setting.

Our findings differ from that reported by Gutman et al., in a study of 75 pre-surgical GBM, they found that visual assessment of proportional contrast enhancement showed worse survival with increasing proportional enhancement with a hazards ratio of 7.745[29]. Proportional enhancement in this study was categorised subjectively as 0-5%, 6-33%, 34-67%, 68-95% and 95-100% by a variety of neuroradiologists, and included the surrounding oedema as part of the whole tumour volume. This differs from the work presented in this study whereby quantitative rather than categorical volumetric assessment was performed, by a single radiologist using a technique, which has previously shown good intra and inter-observer variability [14], and the surrounding T2 signal abnormality/oedema was not included in the whole tumour volume. A larger quantitative volumetric analysis of 94 GBM by the same group also reported increased proportional enhancement was associated with increased mortality ( $p=0.003$ ), but as with the previously study included the perilesional T2 and FLAIR signal abnormality as part of the whole tumour volume [30]. Perez-Beteta et al. assessed the pre-treatment geometry in 117 patients with GBM and reported both increases in tumour volume and contrast enhancing volume were associated with reduced overall survival ( $p=0.034$ , hazards ratio 1.574 and  $p=0.017$ , hazards ratio 1.659), but no assessment of the proportional enhancement of the tumour was made in this study [31].

## Conclusion

This study demonstrates that a measure of proportional enhancement can be derived from conventional pre and post contrast enhanced MR imaging. Whilst  $EnF_{SI}$  demonstrates a significant correlation with EnF derived from DCE-MRI data, both  $EnF_{IAUC60>0}$  and  $EnF_{IAUC60>2.5}$  the two measures are not directly interchangeable. Only  $EnF_{IAUC60>0}$  related to patient survival, with higher values associated with prolonged survival. A similar non-significant trend was seen with the signal intensity based metric of EnF.

## Competing Financial Interests

Both Professor Parker and Dr. Bounaccorsi have additional affiliations with the company Bioxydyn Ltd. The work presented here

is unrelated to this company but the potential conflict of interest by these two co-authors is highlighted.

## Acknowledgement

This work was funded as part of a Cancer Research UK Clinical Research Training Fellowship, reference C21247/A7473 and is an output of Cambridge/Manchester Cancer Imaging Centre.

Study design was conceived by SJM, GJMP and AJ. Data analysis was performed by SJM, GT and GB. The paper was authored by SJM and AJ. All authors reviewed the paper.

## References

- O'Connor JP, Jayson GC, Jackson A, Ghiorghiu D, Carrington BM, et al. (2007) Enhancing Fraction Predicts Clinical Outcome following First-Line Chemotherapy in Patients with Epithelial Ovarian Carcinoma. *Clin Cancer Res* 13: 6130-6135. [[Crossref](#)]
- Mills SJ, Soh C, O'Connor JP, Rose CJ, Buonaccorsi G, et al. (2010) Enhancing Fraction in Glioma and Its Relationship to the Tumoral Vascular Microenvironment: A Dynamic Contrast-Enhanced MR Imaging Study. *AJNR Am J Neuroradiol* 31: 726-731. [[Crossref](#)]
- Mills SJ, Soh C, O'Connor JP, Rose CJ, Buonaccorsi GA, et al. (2009) Tumour enhancing fraction (EnF) in glioma: relationship to tumour grade. *Eur Radiol* 19: 1489-1498. [[Crossref](#)]
- Roberts C, Issa B, Stone A, Jackson A, Waterton JC, et al. (2006) Comparative study into the robustness of compartmental modeling and model-free analysis in DCE-MRI studies. *J Magn Reson Imaging* 23: 554-563. [[Crossref](#)]
- Cao Y, Tsien CI, Nagesh V, Junck L, Haken RT et al. (2006) Clinical investigation survival prediction in high-grade gliomas by MRI perfusion before and during early stage of RT. *International Journal of Radiation Oncology\*Biophysics\*Physics* 64: 876-885.
- Law M, Oh S, Johnson G, Babb JS, Zagzag D, et al. (2006) Perfusion Magnetic Resonance Imaging Predicts Patient Outcome as an Adjunct to Histopathology: A Second Reference Standard in the Surgical and Nonsurgical Treatment of Low-grade Gliomas. *Neurosurgery* 58: 1009-1107. [[Crossref](#)]
- Mills SJ, Patankar TA, Haroon HA, Balériaux D, Swindell R, et al. (2006) Do cerebral blood volume and contrast transfer coefficient predict prognosis in human glioma? *AJNR Am J Neuroradiol* 27: 853-858. [[Crossref](#)]
- Law M, Oh S, Babb JS, Wang E, Inglese M, et al. (2006) Low-Grade Gliomas: Dynamic Susceptibility-weighted Contrast-enhanced Perfusion MR Imaging—Prediction of Patient Clinical Response. *Radiology* 238: 658-667. [[Crossref](#)]
- Law M, Young RJ, Babb JS, Peccerelli N, Chheang S, et al. (2008) Gliomas: Predicting Time to Progression or Survival with Cerebral Blood Volume Measurements at Dynamic Susceptibility-weighted Contrast-enhanced Perfusion MR Imaging. *Radiology* 247: 490-498. [[Crossref](#)]
- Bisdas S, Kirkpatrick M, Giglio P, Welsh C, Spampinato MV, et al. (2009) Cerebral Blood Volume Measurements by Perfusion-Weighted MR Imaging in Gliomas: Ready for Prime Time in Predicting Short-Term Outcome and Recurrent Disease? *AJNR Am J Neuroradiol* 30: 681-688. [[Crossref](#)]
- Hirai T, Murakami R, Nakamura H, Kitajima M, Fukuoka H, et al. (2008) Prognostic value of perfusion MR imaging of high-grade astrocytomas: long-term follow-up study. *AJNR Am J Neuroradiol* 29: 1505-1510. [[Crossref](#)]
- O'Connor JP, Jackson A, Parker GJ, Jayson GC (2007) DCE-MRI biomarkers in the clinical evaluation of antiangiogenic and vascular disrupting agents. *Br J Cancer* 96: 189-195. [[Crossref](#)]
- Haase A (1990) Snapshot FLASH MRI. Applications to T1, T2, and chemical-shift imaging. *Magn Reson Med* 13: 77-89. [[Crossref](#)]
- Thompson G, Cain JR, Jackson A, Mills SJ (2008) Interobserver agreement for cerebral glioma volumetrics on conventional MR imaging.
- Parker GJ, Jackson A, Waterton JC (2003) Automated arterial input function extraction for T1-weighted DCE-MRI.
- Tofts PS (1997) Modeling tracer kinetics in dynamic Gd-DTPA MR imaging. *J Magn Reson Imaging* 7: 91-101. [[Crossref](#)]
- Bland JM, Altman DG (1986) Statistical methods for assessing agreement between two methods of clinical measurement. *Lancet* 1: 307-310. [[Crossref](#)]
- Bland JM, Altman DG (1995) Comparing methods of measurement: why plotting difference against standard method is misleading. *Lancet* 346: 1085-1087. [[Crossref](#)]
- Müller R, Büttner P (1994) A critical discussion of intraclass correlation coefficients. *Statistics in medicine* 13: 2465-2476. [[Crossref](#)]
- Jayson GC, Parker GJ, Mullamitha S, Valle JW, Saunders M, et al. (2005) Blockade of Platelet-Derived Growth Factor Receptor-Beta by CDP860, a Humanized, PEGylated di-Fab', Leads to Fluid Accumulation and Is Associated With Increased Tumor Vascularized Volume. *J Clin Oncol* 23: 973-981. [[Crossref](#)]
- Mullamitha SA, Ton NC, Parker GJ, Jackson A, Julian PJ, et al. (2007) Phase I Evaluation of a Fully Human Anti- v Integrin Monoclonal Antibody (CNTO 95) in Patients with Advanced Solid Tumors. *Clin Cancer Res* 13: 2128-2135. [[Crossref](#)]
- White ML, Zhang Y, Kirby P, Ryken TC (2005) Can tumor contrast enhancement be used as a criterion for differentiating tumor grades of oligodendrogliomas? *AJNR Am J Neuroradiol* 26: 784-790. [[Crossref](#)]
- Pronin IN, Holodny AI, Petraikin AV (1997) MRI of high-grade glial tumors: correlation between the degree of contrast enhancement and the volume of surrounding edema. *Neuroradiology* 39: 348-350. [[Crossref](#)]
- Tofts PS, Benton CE, Weil RS, Tozer DJ, Altmann DR, et al. (2007) Quantitative analysis of whole-tumor Gd enhancement histograms predicts malignant transformation in low-grade gliomas. *J Magn Reson Imaging* 25: 208-214. [[Crossref](#)]
- Hammoud MA, Sawaya R, Shi W, Thall PF, Leeds NE (1996) Prognostic significance of preoperative MRI scans in glioblastoma multiforme. *J Neurooncol* 27: 65-73. [[Crossref](#)]
- Lacroix M, Abi-Said D, Fourney DR, Gokaslan ZL, Shi W, et al. (2001) A multivariate analysis of 416 patients with glioblastoma multiforme: prognosis, extent of resection, and survival. *Journal of Neurosurgery* 95: 190-198. [[Crossref](#)]
- Crawford FW, Khayal IS, McGue C, Saraswathy S, Pirzkal A, et al. (2009) Relationship of pre-surgery metabolic and physiological MR imaging parameters to survival for patients with untreated GBM. *J Neurooncol* 91: 337-351. [[Crossref](#)]
- Ellingson BM, Kim HJ, Woodworth DC, Pope WB, Cloughesy JN, et al. (2014) Recurrent Glioblastoma Treated with Bevacizumab: Contrast-enhanced T1-weighted Subtraction Maps Improve Tumor Delineation and Aid Prediction of Survival in a Multicenter Clinical Trial. *Radiology* 271: 200-210. [[Crossref](#)]
- Gutman DA, Cooper LA, Hwang SN, Holder CA, Gao J, et al. (2013) MR imaging predictors of molecular profile and survival: multi-institutional study of the TCGA glioblastoma data set. *Radiology* 267: 560-569. [[Crossref](#)]
- Wangaryattawanich P, Hatami M, Wang J, Thomas G, Flanders A, et al. (2015) Multicenter imaging outcomes study of The Cancer Genome Atlas glioblastoma patient cohort: imaging predictors of overall and progression-free survival. *Neuro-oncology* 17: 1525-1537. [[Crossref](#)]
- Pérez-Beteta J, Martínez-González A, Molina D, Amo-Salas M, Luque B, et al. (2017) Glioblastoma: does the pre-treatment geometry matter? A postcontrast T1 MRI-based study. *Eur Radiol* 27: 1096-1104. [[Crossref](#)]

**Copyright:** ©2017 Mills SJ. This is an open-access article distributed under the terms of the Creative Commons Attribution License, which permits unrestricted use, distribution, and reproduction in any medium, provided the original author and source are credited.